

Boon Fuei Chang (Primary Contact)
Sheffield University Waste Incineration Centre
Dept. of Chemical and Process Engineering
Sheffield University
Mappin Street
Sheffield, S1 3JD
England
Email: cpp99bfc@shef.ac.uk
Tel: +44 (0)114 2227555
Fax: +44 (0)114 2227501

Professor Jim Swithenbank
Sheffield University Waste Incineration Centre
Dept. of Chemical and Process Engineering
Sheffield University
Mappin Street
Sheffield, S1 3JD
England
Email: j.swithenbank@shef.ac.uk
Tel: +44 (0)114 2227502
Fax: +44 (0)114 2227501

Dr Vida Nasserzadeh Sharifi
Sheffield University Waste Incineration Centre
Dept. of Chemical and Process Engineering
Sheffield University
Mappin Street
Sheffield, S1 3JD
England
Email: v.n.sharifi@shef.ac.uk
Tel: +44 (0)114 2227518
Fax: +44 (0)114 2227501

Professor Noel Warner
40 High House Drive
Rednal
Birmingham
B45 8ET
England

Development of a Liquid Metal Based Fuel Gas Scrubbing System

Keywords: Packed Bed Scrubber, Liquid Metal, Desulphurisation, Particulates Removal

Introduction

Present integrated gasification combined cycle (IGCC) systems demonstrate high system efficiency and impressive environmental performance, giving these systems an edge over conventional pulverized fuel power stations. However, problems of high capital costs, low reliability and poor operational flexibility (UK DTI, 1998) need to be overcome to make IGCC systems more attractive. This necessitates improvement in various areas of gasification systems, a major one being hot fuel gas clean-up.

Current hot gas clean-up methods focus on the use of metal oxide sorbents for sulphur removal and the utilisation of ceramic barrier filters for particulate cleaning. In contrast, this research project adopts an unconventional approach to fuel gas cleaning technology, incorporating molten tin as scrubbing medium for the removal of H₂S and solid particulates.

The concept of using liquid metals for gas desulphurisation is not entirely new, this being documented in the mid-80s by researchers in Germany. Schürmann (1984) showed that H₂S removal is achievable with molten tin and that there was a possibility to combine sulphur and dust removal in a scrubber incorporating liquid tin. Hedden *et al.* (1986) investigated the desulphurisation of manufactured gases with molten tin in small-scale reactors. Based on their experimental findings, they proposed a process in which the hot fuel gas is cleaned of sulphur and fine dust by a molten tin spray. The SnS solid product is next treated with oxygen and SO₂

giving SnO₂ and elementary sulphur. This is then followed by SnO₂ reduction in a purified fuel gas stream to regenerate the liquid tin.

However, it can be shown that the degree of sulphur removal in the process put forward by Hedden *et al.* is limited by thermodynamic constraints (Warner, 2000). Low activity of dissolved sulphur in the molten tin has to be maintained for effective sulphur removal. In the process proposed by Warner, a liquid tin based hot gas scrubbing system addresses this issue. High temperature sulphur removal takes place in a non-wetting, liquid tin irrigated moving packed bed. Sulphur removal occurs via absorption of hydrogen sulphide into molten tin.



The reaction should proceed unimpeded as long as the dissolved sulphur in the molten tin is below the saturation level with respect to tin sulphide. To maintain a sufficiently low tin sulphide activity in the molten tin, continuous tin regeneration is effected by external treatment with liquid zinc producing saleable high quality zinc sulphide (Warner, 1997). In addition to gas desulphurisation, simultaneous solid particulate removal is possible in the packed bed. Molten tin having high surface energy exhibits non-wetting droplet flow on the packing surface, potentially giving good inertial capture of solid particulates by the packed bed from the gas stream.

This paper presents the results of cold test studies conducted on a non-wetting flow packed bed scrubber and shows the application of these data to the design of a small scale molten tin irrigated high temperature scrubber. The system in the current study incorporates a fixed bed rather than a moving bed, nevertheless the results will be useful to the subsequent development of a moving packed bed scrubber.

Objective

The objective of this research project is to perform studies on an analogous room temperature packed bed scrubber operating under non-wetting conditions, providing insight and understanding towards the development of a high temperature packed bed gas scrubber irrigated by molten tin.

Approach

A series of cold tests were conducted on a Perspex model of the gas scrubber operating under non-wetting flow conditions analogous to liquid metal flow. The aims of the cold tests are twofold. Firstly, to study the operational hydraulics of the packed column under non-wetting conditions in order to derive suitable operating parameters and to finalise dimensions for the high temperature system. Secondly, to investigate gas absorption and particulate removal performance under non-wetting flow conditions. In addition, simulation studies on particulate removal in the packed bed under non-wetting flow were carried out using FLUENT.

Project Description

Due to their high surface free energies, liquid metals generally exhibit non-wetting type of flow on solid surfaces (Zisman, 1964). This non-wetting flow behaviour was to be simulated at room conditions during the cold tests. The room temperature system was to be irrigated by water for convenience. Hence the selected solid packing material has to be hydrophobic i.e. water-repelling to set up an analogous non-wetting room temperature system. This meant that the contact angle of water on the selected solid material has to be greater than 90°. With this in mind, polyethylene spheres as well as paraffin waxed glass spheres were selected as packings for the

room temperature model scrubber. The contact angle of water on paraffin surface is 110° while the average contact angle of water on polyethylene surface is 95° (Adamson and Gast, 1997).

Room-condition tests in air-water system were performed on an 8 cm internal diameter Perspex column with approximately 19 cm packed bed height. The internal wall of the Perspex column was waxed. Two types of packings were used: 9.5 mm solid high density polyethylene spheres and 10 mm solid soda lime glass spheres treated with paraffin wax. Details are given in Table 1.

The following cold tests are discussed in this paper:

- Flow visualisation studies
- Packed column operational hydraulics:
 - Flooding capacity
 - Liquid holdup
- Liquid circulation via gas lift
- Particulate removal

Results

Flow Visualisation

High-speed digital imaging was performed with a Redlake MotionScope PCI Series monochrome camera (Model PCI 8000 S) to study the non-wetting flow of water on the packing surface. The spherical packing configurations which encourage droplet flow formation were identified. These are sites with a single packing sphere having an immediate space below it and sites at which two or three spheres contact one another. At all these locations, the water droplet grows in size as more water is held up, the additional water flowing either from the top or from within the packed bed. When the droplet diameter reaches approximately 4 mm, it becomes unstable due to its weight and is displaced downwards. This demonstrates the mobility of the static holdup due to the tendency of water to form droplets rather than a spreading film on the hydrophobic surface of polyethylene and paraffin waxed glass beads.

At high water flowrates, the frequency of droplet formation is sufficiently high such that the individual droplets flow so close to one another that a rivulet flow about 3 to 4 mm width is formed. Generally, rivulet flow became more pronounced at higher fluid flowrates and this is especially so at higher liquid flowrates.

The droplets hanging from the bottom point of the spherical beads are examples of pendent (or hanging) droplets. The static equilibrium of the pendent droplet hanging from the bead bottom surface is governed by the balance between surface tension and the gravitational force. Based on this principle, the surface tension of a liquid pendent drop is given by the following equation (Adamson, 1976):

$$\gamma_L = \frac{\Delta\rho g d_e^2}{H} \quad (2)$$

Rearranging:
$$H = \frac{\Delta\rho g d_e^2}{\gamma_L} \approx \frac{\rho_L g d_e^2}{\gamma_L} \quad (3)$$

where

H	= a shape dependent quantity (-)
$\Delta\rho$	= density difference between liquid and gas phase ρ_L (kg/m^3)
ρ_L	= liquid density (kg/m^3)
g	= gravitational acceleration (m/s^2)

For a hydrophobic surface, a pendent water droplet is expected to adopt a pearl-like shape i.e. with d_s less than d_e (see Figure 1). Hence since $S = d_s/d_e$, S is expected to be less than 1. From the tables of $1/H$ versus S values of Niederhauser and Bartell (1950), for an S value less than 1, the corresponding $1/H$ value has to be greater than 0.30586.

$$\therefore d_e < \left(\frac{\gamma_L}{0.30586 \times \rho_L g} \right)^{1/2} \quad (4)$$

Applying inequality 4 with the physical properties of water at room conditions ($\gamma_L = 73.49 \times 10^{-3}$ N/m; $\rho_L = 1001.29$ kg/m³) the equatorial diameter, d_e was worked out to be less than 4.9 mm. The experimentally observed maximum water droplet size on the spherical packings before falling off the solid surface is approximately 4 mm. This agrees with the calculated range of equatorial diameter of less than 4.9 mm.

Since the hot scrubber incorporates spherical ceramic packings dimensionally similar to the polyethylene and waxed glass spheres, the drip tip at the bottom surface of the packing would be dimensionally alike as well. Therefore, the pendent droplet of molten tin at the bottom tip of a ceramic sphere would be expected to also conform to inequality 4. Using the physical properties of molten tin at a typical operating temperature, say 350°C ($\gamma_L = 0.549$ N/m; $\rho_L = 6908$ kg/m³) (Iida and Guthrie, 1988) the equatorial diameter d_e was worked out to be less than 5.1 mm. Therefore the maximum molten tin droplet size in the packed bed of the hot scrubber would be expected to be approximately 5 mm.

The velocity of the droplets measured in this work assuming vertical downward movement only ranged from 10 mm/s to 37 mm/s.

Flooding Capacity

Flooding determines the maximum capacity and marks the onset of instability in the operation of a packed column. The liquid fills the column and there may be pronounced liquid entrainment in the outlet gas. Hence for design purposes, it is desirable to know the upper limits of gas and liquid flow rates in a packed column dictating the onset of flooding to ensure that the column operates within a safe operating range.

The flooding capacity of the Perspex column operating under non-wetting flow was investigated. While maintaining a constant water flowrate, the air flowrate was increased in a stepwise manner until flooding was achieved, the pressure drops being noted for each air flowrate after allowing for stabilization of the flow. Flooding was established based on a combination of graphical and visual indicators: a sudden steep change in the gradient of bed pressure drop versus air mass velocity plots, accumulation of water throughout the whole packed bed up till the upper surface of the bed, and wild fluctuations in pressure drop readings as flooding sets in. The flooding points obtained for the water-irrigated packed bed made up of polyethylene spheres as well as paraffin waxed glass spheres were obtained and are plotted in Figure 2. These flooding points are found to be clearly displaced above the now classical generalised flooding correlation of Sherwood, Shipley and Holloway (1938). Sherwood *et al.*'s (1938) correlation was developed using a packed bed of carbon Raschig rings irrigated by water and aqueous organic solutions i.e. essentially wetting systems. On the same plot in Figure 2, the other non-wetting flooding data available in the literature and most importantly, which includes liquid metal irrigated systems has been included for comparison. Good agreement in flooding capacity is demonstrated by all the non-wetting systems. This is despite the fact that the density and surface tension of water (1001

kg/m³ and 73 dynes/cm respectively at 15°C) are markedly lower than that of the liquid metals (13591 kg/m³ and 488 dynes/cm for mercury at 15°C). However all the systems have one thing in common i.e. the liquid does not wet the solid surface as the contact angle of the liquid with the solid surface is greater than 90° as follows (Adamson and Gast, 1997): Water on polyethylene surface: 95°; Water on paraffin surface: 110°; Mercury on glass: 128-148°. This implies that due to the non-wetting condition in the packed bed, the liquid that is held up within the column is lower than that of a wetting system under the same conditions of fluid flowrates and therefore allowing a greater flooding capacity. This in turn suggests that non-wetting systems can sustain higher fluid velocities than conventional wetting systems before the onset of flooding, hence a smaller column would be viable for a given set of fluid volume flowrates. Also, from Figure 2 it can be seen that the flooding capacity of the non-wetting systems is in general slightly higher for larger contact angles i.e. the more pronounced the non-wetting behaviour.

The hot gas scrubber incorporates 9.5 mm spherical ceramic packings and it is irrigated by molten tin. The flooding capacity of the hot gas scrubber is thus expected to conform to the generalised flooding correlation of the non-wetting systems in Figure 2. Based on this graphical correlation, the flooding gas velocity of the hot gas scrubber can be determined for a given molten tin flowrate and a safe gas-liquid operating range can then be obtained.

Liquid Holdup

In a packed column, the liquid holdup refers to the liquid retained in the bed of packings i.e. films or droplets on the surface of the packings or the liquid trapped in the interstitial space between the packings. The total liquid holdup is the total amount of liquid on the packing under dynamic conditions i.e. the sum of the static holdup and dynamic holdup. Static holdup is the volume of liquid per volume of packing that remains in the packed bed that has been fully wetted after the gas and liquid flows have stopped and the bed has drained. The fraction that drains out is the dynamic holdup.

The static and dynamic liquid holdups for the Perspex column were determined. For both holdup measurements, sufficient time was allowed for the flow through the column to stabilise. Once this was achieved, both the air and water supplies were cut off simultaneously. The bed was allowed to drain until water drainage became negligible. The dynamic holdup was determined by weighing the amount of water that drained from the bed. An earlier determined portion of the dynamic holdup contributed by water accumulated in the top water distributor and the bottom reservoir was deducted, giving the actual dynamic holdup for the packed bed. The static holdup was determined by the difference in the weight of the dry packings and that of the wet packings after the bed has drained.

The results of the liquid holdup tests using water-irrigated polyethylene beads are illustrated in Figures 3 and 4. There was a small but definite decrease in static holdup as water flowrate increases. The static holdup varied from an average value of 3.46 to 3.03 vol % of packing as water velocity increased from 0.35 to 0.87 cm/s. Based on conventional wetting systems (water irrigation of ceramic and carbon packings), it was previously reported that static holdup is independent of variations in gas and liquid flowrates but it is a function of the nature of the packing and the liquid physical properties (Shulman *et al.*, 1955a). Static holdup is thought to be made up of very stagnant pools protected in the packing interstices, replaced very slowly by fresh liquid. The liquid in the static hold-up rapidly becomes equilibrated with the adjacent gas while it is only displaced very slowly by fresh liquid. Hence, it was deduced that the semi-stagnant static holdup is relatively ineffective to mass transfer in an absorption process (Shulman *et al.*, 1955a). In contrast, the results of this work demonstrate that the static holdup for a packed column operating under non-wetting flow conditions is actually affected by water flowrates. A

likely reason for this difference is that the water droplets held in the interstices of the packings in non-wetting flow are more easily displaced at higher water flowrates than the semi-stagnant pools formed in wetting flow conditions. This is further supported by the observed mobility of static holdup in the high speed video footage. The results herein suggests that the static holdup in a non-wetting flow packed bed system has a relatively more effective contribution to mass transfer in a gas absorption process than a conventional wetting system. The dependence of static holdup on liquid rate found in this work is in agreement with reported static holdup trend for liquid metal irrigation. Both Warner (1959) and Standish (1968b) reported that the static holdup for mercury irrigated steel and porcelain rings slightly decreased with increasing mercury flowrates.

The dynamic holdup for the water irrigated polyethylene packings was found to increase with both the air and water rates, with a greater dependence on the liquid rate. The onset of flooding is accompanied by a sudden rapid rise in dynamic holdup. This observation generally agrees with the dynamic holdup trend of wetting systems incorporating aqueous solutions and organic liquids (Shulman *et al.*, 1955b). The dynamic holdup for liquid metal irrigation also increased with both gas (Warner, 1959) and liquid (Standish, 1968a) rates. In an absorption process, the dynamic hold-up is effective to mass transfer rate as it is continuously replaced and regenerated, hence providing the residence time for gas-liquid interfacial contact.

Hence the total liquid holdup i.e. the sum of both the static and dynamic holdups increased with both air and water flow-rates with the latter exerting a greater influence as described by the following correlation:

$$h_T = 265(v_G^{0.178})(v_L^{0.580}) \quad (5)$$

where h_T = total liquid holdup (vol. %)
 v_G = air superficial velocity (m/s)
 v_L = water superficial velocity (m/s)

The coefficient of determination, R^2 for the above correlation is 0.88. The parity plot is shown in Figure 5.

Despite the pronounced differences in liquid density and surface tension, the liquid holdup trends especially that of the static holdup found in this work for water irrigated polyethylene packings are in accordance with those reported for liquid metal irrigation. This suggests that for a packed column operating under non-wetting conditions, liquid-solid packing contact angles exert a dominating influence not only on the flooding capacity but on the liquid holdup as well.

Gas Lift

Molten tin is to be circulated through the hot gas scrubber. The high temperature conditions, the highly corrosive nature of molten tin as well as the presence of solids in suspension render most conventional mechanical pumps unsuitable for this operation. A simple and yet reliable method is provided by the gas lift pump. The gas involves no moving parts that are susceptible to erosion or wear, and only requires a compressed gas supply as the transporting agent. Compressed gas is injected at the bottom of the gas lift riser forming gas bubbles in the liquid. The gas bubbles reduce the density of the overall gas/liquid mixture in the riser compared to the liquid alone, providing a buoyancy force. Consequently, the gas/liquid mixture rises upwards where it is discharged at the top of the riser.

Water circulation through the Perspex packed column via a small air lift pump was investigated. The dimensions of the air lift are as follows: 1.59 cm internal diameter piping for riser and downcomer, 45 cm lift, 65 cm submergence hence 0.59 submergence ratio (i.e. submergence to

total height of air lift). 3 different gas injectors were tested: a 5 mm i.d. longitudinal injector, a radial injector with four circumferentially equidistant 2.54 mm air ports and a radial injector with twelve 2.54 mm air ports arranged in 3 rows (4 to one row, circumferentially equidistant). The water discharged at the top of the air lift was collected in a recorded period of time and then weighed. Three readings were taken for each air flowrate and the average water flowrate determined. It was found that there was negligible difference in the pumping performance of the air lift with these 3 different air injectors as shown in Figure 6. This result is in contrast to reported improved pump efficiency with multiport injectors in a larger air lift (Morrison *et al.*, 1987).

The air lift experimental data obtained in this work is plotted on the axes of Zenz graphical correlation for the design of air lift pumps (Zenz, 1993). The ordinate includes factors of fluid density, viscosity and surface tension relative to those of water to enable the application of the air lift graphical correlation on other fluids to be pumped apart from water. The experimental data curve obtained from the tested room temperature air lift and plotted on Zenz's axes was used to predict the pumping capacity of the nitrogen gas lift on molten tin in the hot scrubber.

Particulate Removal

Particulate removal performance of the water-irrigated column packed with polyethylene spheres was investigated using a glass dust laden air stream. The glass dust consists of spherical particles ranging from 1.5 to 35 μm with a uniform density of 1100 kg/m^3 . The particle size distribution of the glass dust was determined on the AccuSizer 780A Particle Sizing System. The size distribution of the glass dust resembles very closely a log-normal distribution with mass median diameter of 10.2 μm and geometric standard deviation of 1.8.

Figure 7 illustrates the experimental setup used to determine the total efficiency. Malvern Instruments' Qspec Dry Powder Feeder was used for dust loading into the inlet air stream. The penetrating glass dust was filtered from the exiting air stream using a Whatman in-line cartridge filter with 1.0 μm particle retention capability. This filter type was chosen for its exceptionally high particle retention and high loading capacity. Isokinetic sampling was not feasible on this small scale scrubber due to the small flow area of the exit line employed (about 1.5 cm internal diameter). The duration of each test run was approximately 10 to 15 minutes. At the end of the each run, the cartridge filter was removed from its housing, dried in the oven and weighed. The total efficiency of the scrubber, E_T is determined gravimetrically as follows:

$$E_T = 1 - \frac{m_{out}}{m_{in}} \quad (6)$$

where m_{out} = mass of unseparated dust retained in filter (g)
 m_{in} = mass of dust fed into the scrubber (g)

The penetrating dust particle size distribution was determined to obtain the grade efficiency. The dust in the exiting air stream was collected into water in an impinger. Samples of the solid in suspension from the impinger are then run through the AccuSizer 780A Particle Sizing System to determine the particle size distribution. The experimental setup used is illustrated in Figure 8. By controlling the needle valve downstream of the impinger, it was possible to operate at the same column pressure drop with the same operating fluid flowrates as when the filter was in place. This ensured that dust collected in the impinger would be representative of the dust collected on the filter at the same operating fluid flowrates. One impinger was found to be sufficient for full collection of the dust in the exit air stream. The grade efficiency, $G(x)$ is determined gravimetrically as follows:

$$G(x) = 1 - (1 - E_T) \frac{\omega_{out,i}}{\omega_{in,i}} \quad (7)$$

where $\omega_{out,i}$ = mass fraction of unseparated dust retained in filter in size range i
 $\omega_{in,i}$ = mass fraction of dust fed into the scrubber in size range i

The dust feed rate was adjusted at each air flowrate to give an average inlet dust concentration ranging from approximately 500 to 3000 ppmw. The operating air superficial velocity ranged from 18.49 to 29.65 cm/s (measured downstream of column at atmospheric pressure) while the water superficial velocity ranged from 0.35 to 0.87 cm/s. The variation of total collection efficiency with air and water flowrates as well as inlet dust concentration is shown in Figures 9 and 10.

Total efficiency E_T increases with air and water flowrates as well as inlet dust concentration. At higher air or water flowrates, the total liquid holdup in the packed bed increases as shown in the earlier liquid holdup tests. The droplets and rivulets in the bed increase, therefore improving the deposition of solid particulates through inertial capture and direct interception. High dust loading gives better overall dust separation in the water irrigated packed bed. This is because the moisture encourages agglomeration of dust particles, resulting in larger overall particle sizes and hence improved dust separation from the air stream. The importance of the presence of water in the packed bed to prevent re-entrainment of dust particles into the air stream is demonstrated by the experimental data curve at zero water flowrate in Figure 10. At dry bed condition, dust separation decreases with increasing dust concentration. At the start, the dust introduced into the bed will stick to the clean packing surfaces mainly due to electrostatic force generated between the dry dust and the polyethylene spheres. The tendency for electrostatics buildup is high due to the relative positions of glass and polyethylene in the triboelectric series. However, the available clean packing surfaces decline rapidly as more dust enters the column. Having found no ways of being deposited and retained in the packed bed, the additional dust is swept along with the air stream out of the column. The dry bed has only a certain dust retention capacity. Hence as the inlet dust concentration increases, a higher proportion of the dust penetrates and escapes the packed bed, reducing the overall separation efficiency.

Using multiple linear regression analysis, the following correlation is obtained expressing the total efficiency in terms of air and water superficial velocities as well as inlet dust concentration. The corresponding value of the coefficient of determination, R^2 for the correlation is 0.80. The parity plot is shown in Figure 11.

$$E_T = 103.20(v_G^{0.025})(v_L^{0.013})(C_p^{0.008}) \quad (8)$$

where v_G = air superficial velocity (m/s)
 v_L = water superficial velocity (m/s)
 C_p = inlet dust concentration (ppmw)

The water-irrigated scrubber demonstrates impressive dust removal performance with total separation efficiency ranging from 95.5 to 99.6%. Cut sizes approaching submicron is achievable as shown by the grade efficiency plots in Figure 12. Compared to the cold scrubber, an even better dust removal performance can be expected of the molten tin irrigated hot scrubber. This is because besides the inertial capture of solid particulates from the gas stream by molten tin droplets and rivulets, the adhesiveness of ash and char particles at elevated temperatures will also encourage deposition and retention on the packing surfaces.

Application

Results from the cold tests have provided insight and understanding to the development of a liquid metal irrigated packed bed scrubber. The design of the hot gas scrubber has been finalised and its construction completed.

Future Activities

The next phase of the project will be to investigate the performance of the molten tin irrigated packed bed scrubber in removing H₂S and solid particulates from a simulated hot fuel gas.

References

1. Adamson, A.W. (1976) *Physical Chemistry of Surfaces*. 3rd edition. New York, John Wiley & Sons.
2. Adamson, A.W. and Gast, A.P. (1997) *Physical Chemistry of Surfaces*. 6th edition. New York, John Wiley & Sons, Inc.
3. Hedden, K. *et al.* (1986) *Desulfurization of manufactured gases with liquid metals: Proceedings of the 1986 International Gas Research Conference held at Toronto, Ont, Canada*.
4. Iida, T. and Guthrie, R.I.L. (1988) *The physical properties of liquid metals*. Oxford, Clarendon Press.
5. Kukarin, A.S. and Kitaev, B.I. (1962) *Izv. V.U.Z.Chern. Met.*, 12, 20. Cited in: Standish, N. (1973) On the flooding criteria for liquid metals. *Chemical Engineering Science*, 28, 1906-1907.
6. Morrison, G.L. *et al.* (1987) Experimental analysis of the mechanics of reverse circulation air lift pump. *Ind. Eng. Chem. Res.*, 26, 387-391.
7. Niederhauser, D.O. and Bartell, F.E. (1950) *Report of Progress – Fundamental Research on the Occurrence and Recovery of Petroleum*. Baltimore, American Petroleum Institute, The Lord Baltimore Press. Cited in: Adamson, A.W. (1976) *Physical Chemistry of Surfaces*. 3rd edition. New York, John Wiley & Sons.
8. Schürmann, B. (1984) Untersuchungen über die Gasreinigung durch geschmolzene Stoffe und Entwicklung eines entsprechenden Verfahrens (Studies of gas purification by molten materials and development of an appropriate method). *Fortschritt-Berichte der VDI-Zeitschriften Reihe 3: Verfahrenstechnik*, 85.
9. Sherwood, T.K., Shipley, G.H. and Holloway, F.H. (1938) Flooding velocities in packed columns. *Industrial Engineering Chemistry*, 30(7), 765-769.
10. Shulman, H.L. *et al.* (1955a) Performance of packed columns I. Total, static and operating holdups. *Journal of AIChE*, 1(2), 247-253.
11. Shulman, H.L. *et al.* (1955b) Performance of packed columns III. Holdup for aqueous and nonaqueous systems. *Journal of AIChE*, 1(2), 259-264.
12. Standish, N. (1968a) Dynamic hold-up in liquid metal irrigated packed bed. *Chemical Engineering Science*, 23, 51-56.
13. Standish, N. (1968b) Some observations on the static hold-up of aqueous solutions and liquid metals in packed beds. *Chemical Engineering Science*, 23, 945-947.

14. Standish, N. (1973) On the flooding criteria for liquid metals. *Chemical Engineering Science*, 28, 1906-1907.
15. Szekely, J. and Mendrykowski, J. (1972) On the flooding criteria for liquids with high density and high interfacial tension. *Chemical Engineering Science*, 27, 959-963.
16. UK Department of Trade and Industry (1998) *Technology Status Report-Gasification of Solid and Liquid Fuels for Power Generation*. DTI's Cleaner Coal Technology Programme.
17. Warner, N.A. (1959) Liquid metal irrigation of a packed bed. *Chemical Engineering Science*, 11(3), 149-160.
18. Warner, N.A. (1997) Zinc-based clean technology for desulphurisation in advanced power generation. Report No. COAL R127, UK DTI's Coal Research and Development Programme managed by Energy Technology Support Unit.
19. Warner, N.A. (2000) Private communication-*Theoretical framework for liquid-metal based coal gasification (draft)*.
20. Zenz, F.A. (1993) Explore the potential of air-lift pumps and multiphase. *Chemical Engineering Progress*, 89(2), 51-56.
21. Zisman, W.A. (1964) Relation of equilibrium contact angle to liquid and solid constitution. In: Gould, R.F. (ed) *Contact angle, wettability and adhesion. Advances in Chemistry Series*, 43. Washington D.C., American Chemical Society.

Figures and Tables

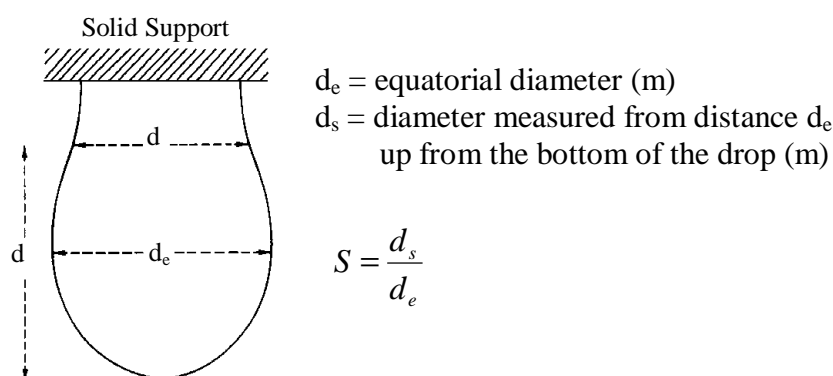
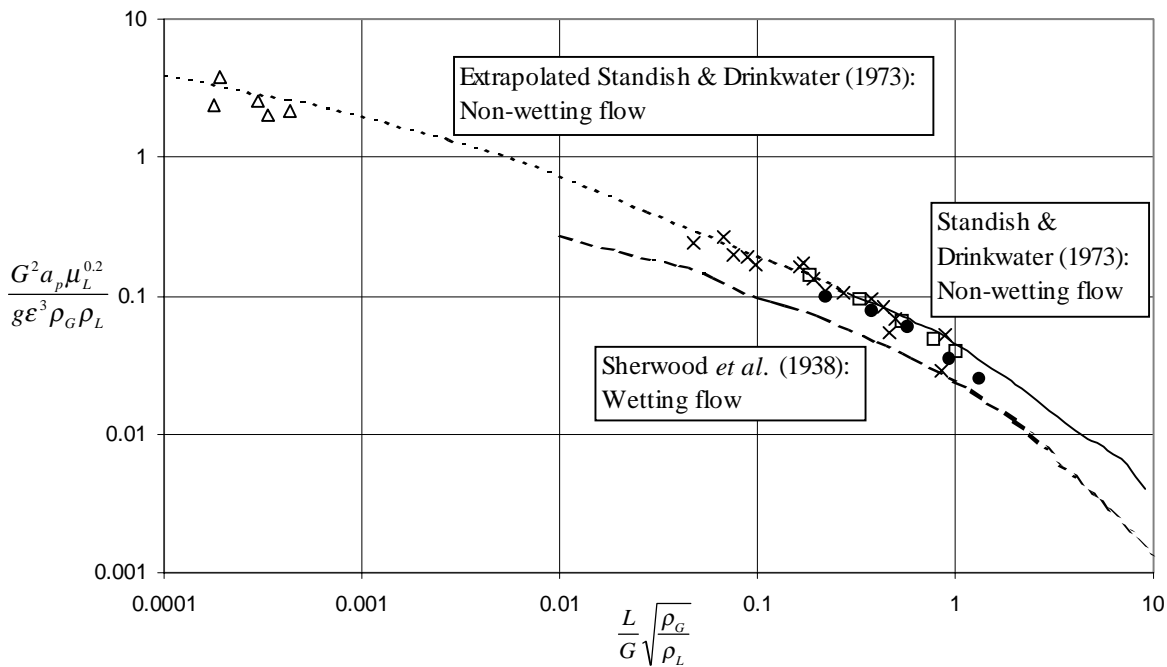


Figure 1 Pendent (or hanging) drop.



- This Work: Water irrigated polyethylene beads
- ◻ This Work: Water irrigated paraffin waxed glass beads
- Standish & Drinkwater (1973): Water irrigated waxed packings
- Extrapolation of Standish & Drinkwater's data (1973)
- Sherwood, Shipley & Holloway (1938): Water/Aqueous solution irrigated unwaxed packings
- × Szekely & Mendrykowski (1972): Mercury irrigated glass and ceramic packings
- △ Kukarin & Kitaev (1962): Woods Metal irrigation

Nomenclature:

- G = gas mass velocity (kg/m²s)
- L = liquid mass velocity (kg/m²s)
- g = gravitational acceleration (m/s²)
- a_p = specific surface area of packed bed (m²/m³)
- ε = bed porosity (-)
- μ_L = liquid viscosity (cP)
- ρ_G = gas density (kg/m³)
- ρ_L = liquid density (kg/m³)

Figure 2 Comparison of flooding points under non-wetting and wetting conditions in a packed column.

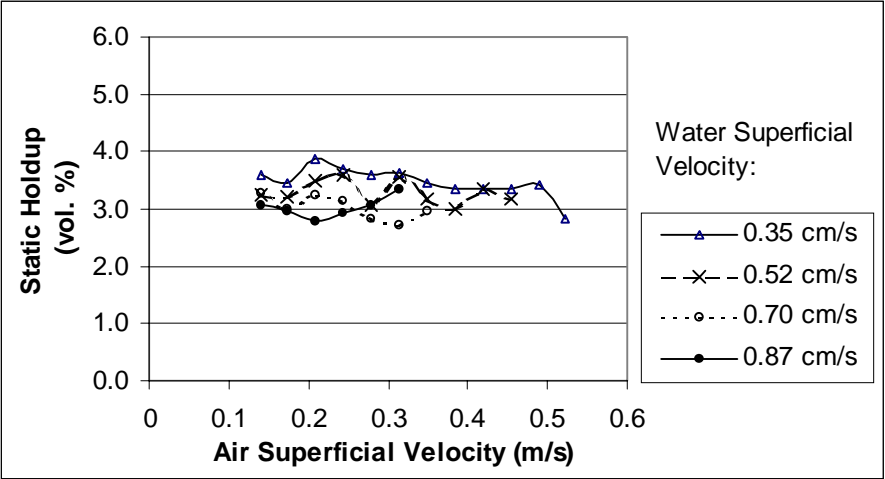


Figure 3 Variation of static liquid holdup with air and water flowrates.

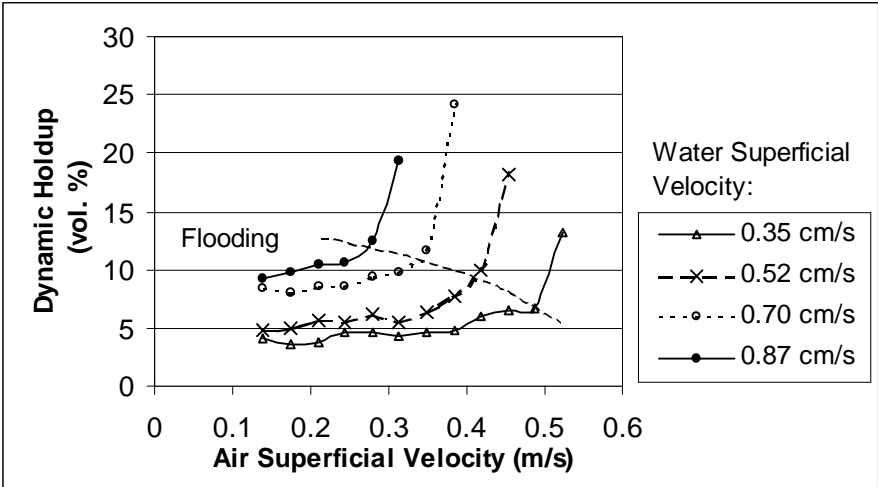


Figure 4 Variation of dynamic liquid holdup with air and water flowrates.

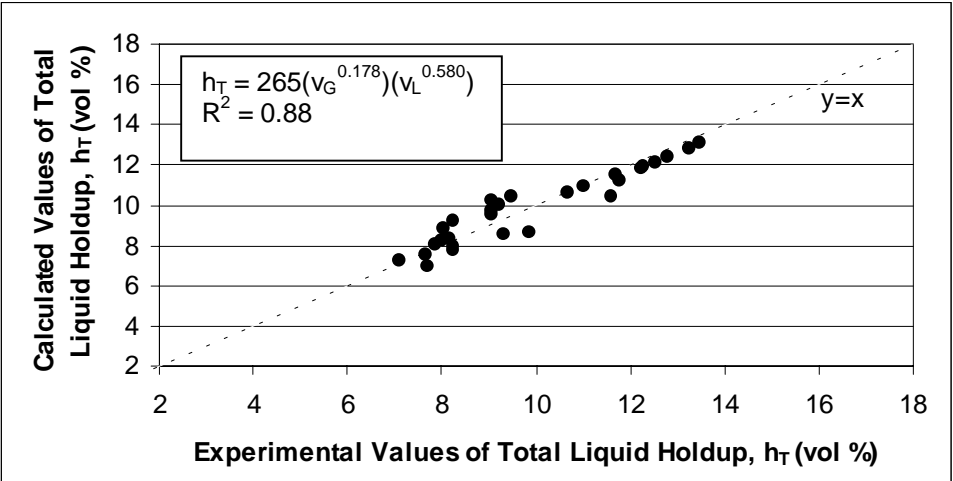


Figure 5 Comparison of calculated and experimental values of total liquid holdup.

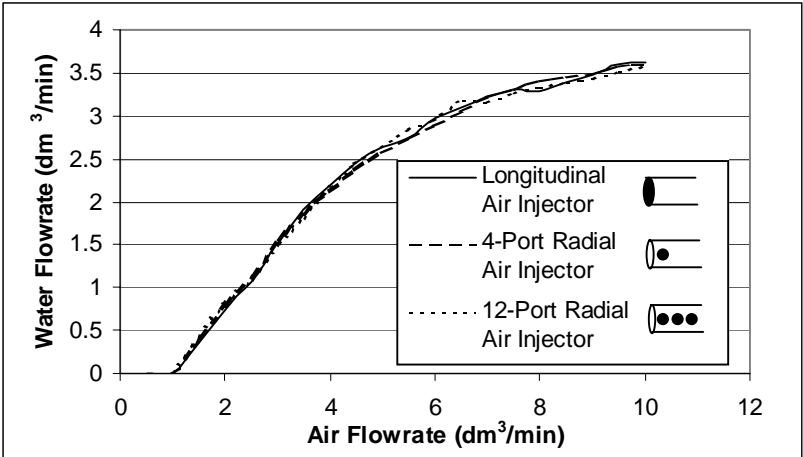


Figure 6 Air lift performance chart with varying injectors.

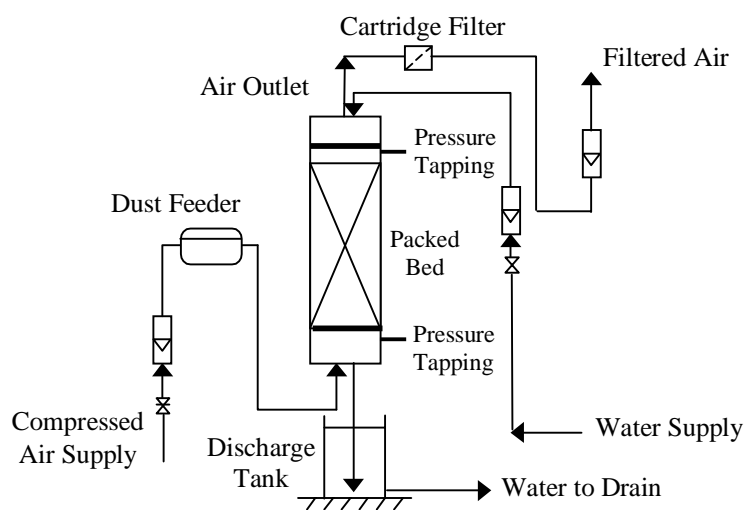


Figure 7 Experimental setup to determine total efficiency of dust removal.

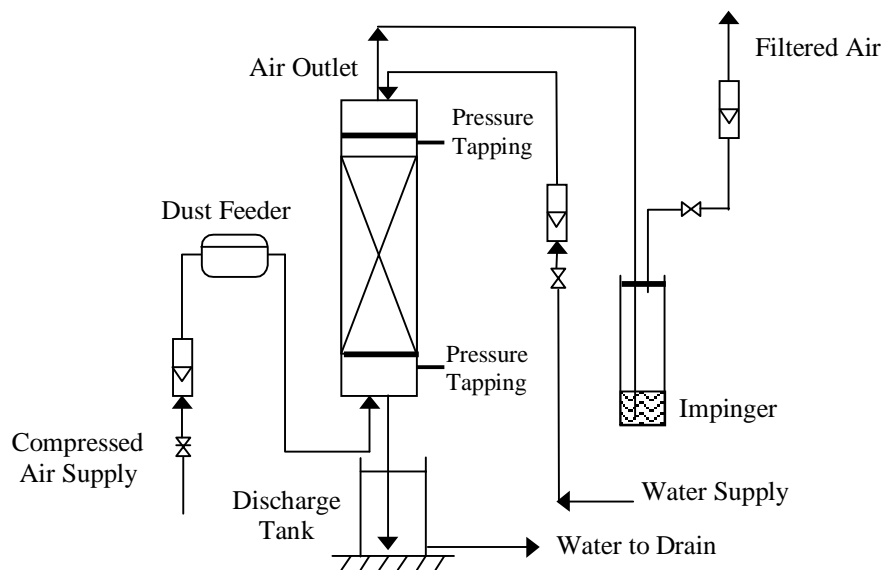


Figure 8 Experimental setup to determine grade efficiency of dust removal.

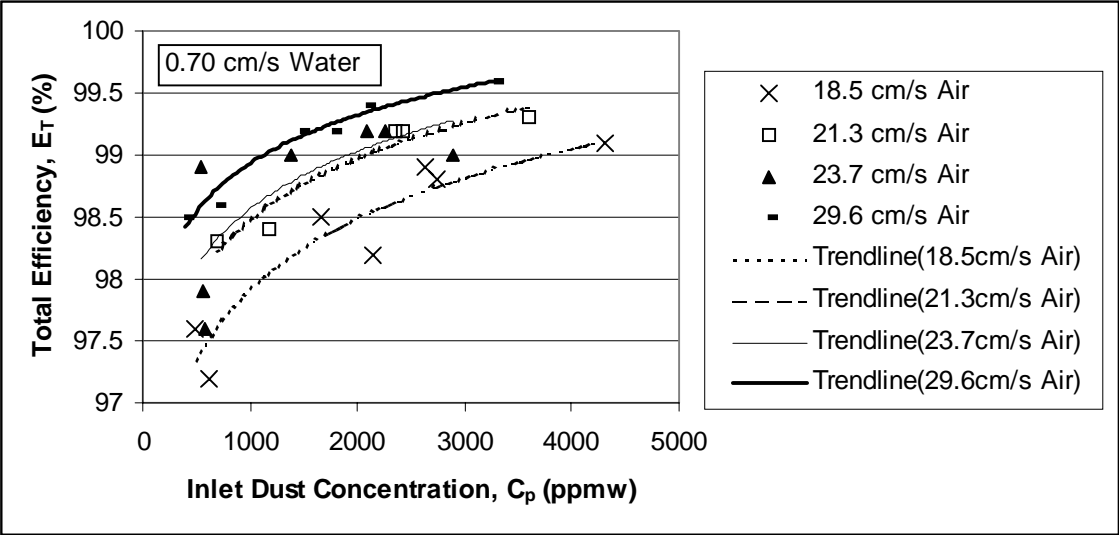


Figure 9 Variation of total efficiency with inlet dust concentration and air flowrate.

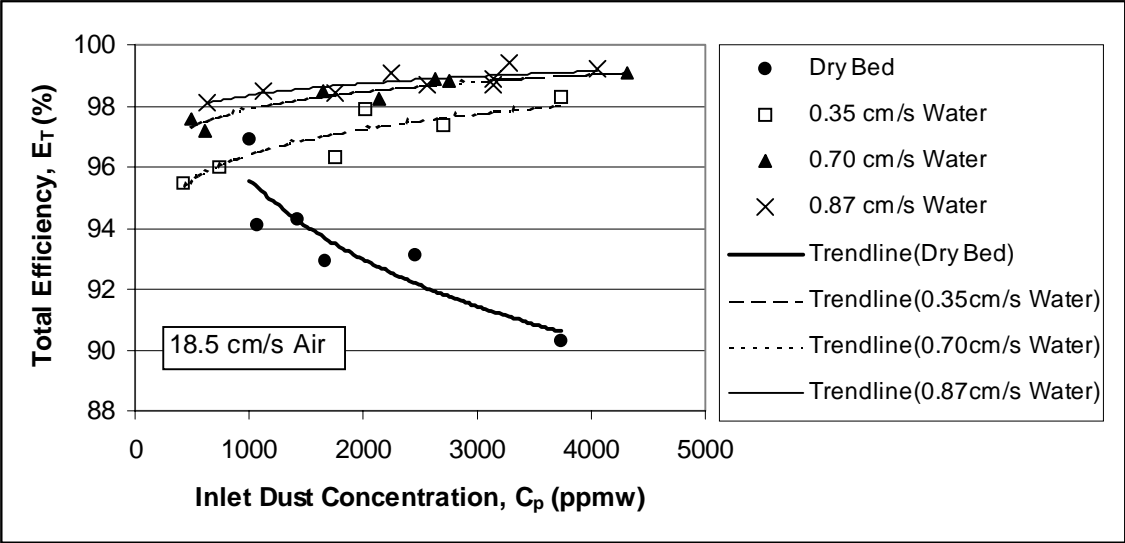


Figure 10 Variation of total efficiency with inlet dust concentration and water flowrate.

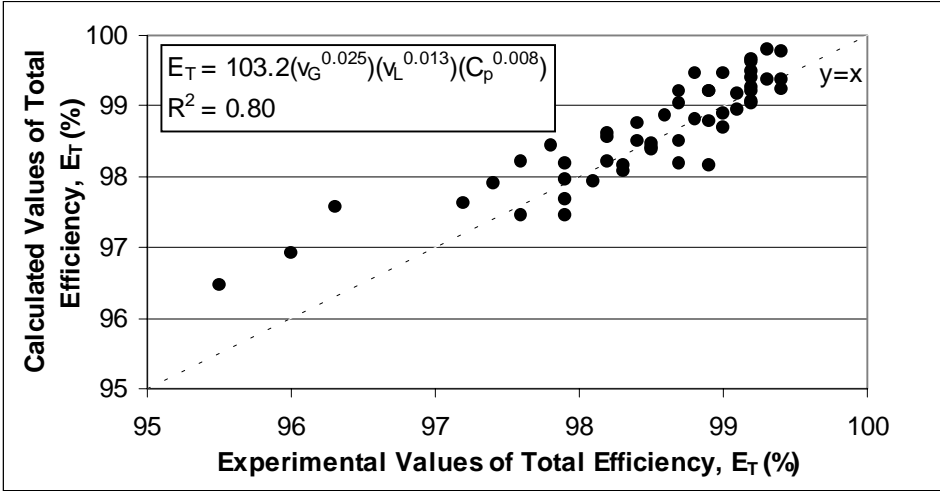


Figure 11 Comparison of calculated and experimental values of total efficiency.

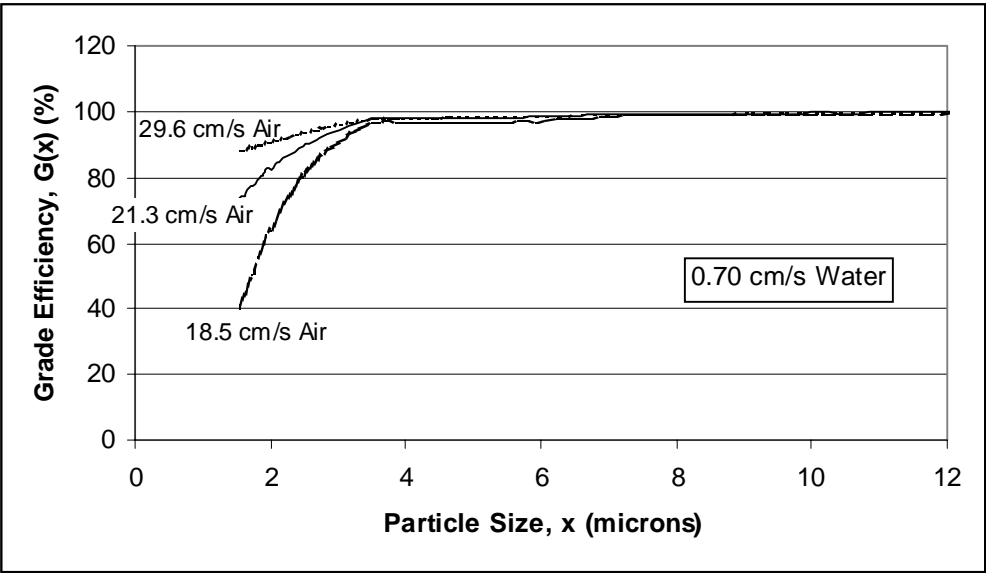


Figure 12 Grade efficiency curves.

Table 1 Characteristics of packings used.

Packing	Diameter (mm)	Specific Gravity	Specific Surface Area (m ² /m ³)	Porosity	Column to Packing Diameter Ratio
Solid polyethylene beads	9.5	0.96	630	0.45	8.4
Solid glass beads treated with paraffin wax	10.0	2.5	600	0.45	8.0